Double-Clad Structures and Proximity Coupling for Diode-Bar-Pumped Planar Waveguide Lasers

C. L. Bonner, T. Bhutta, D. P. Shepherd, and A. C. Tropper, *Member, IEEE*

***Abstract*—We report, for the first time, fabrication of double-clad planar waveguide structures and their use for multiwatt, diode-bar-pumped, planar waveguide lasers based on Nd^{3+}- and Yb^{3+}-doped YAG. The direct-bonded, five-layer structures of sapphire, YAG, and rare-earth-doped YAG have sufficient numerical aperture to capture the fast-axis divergence of a diode bar by proximity coupling with no intervening optics, leading to very simple and compact devices. The restriction of the doped region to the central core leads to diffraction-limited laser output in the guided direction. We also show that the direct-bonding fabrication process can lead to a linearly polarized output.**

***Index Terms*—Laser resonators, lasers, laser modes, waveguides, waveguide theory.**

I. Introduction

LASER MEDIA with high-aspect-ratio slab geometries are known to have improved thermal limitations in comparison to cylindrical rods [1]. This makes them attractive for high-power laser systems where the accompanying large thermal load can cause optical distortions and even fracture. Planar thin-film waveguides can be seen as an extreme case of the slab geometry with typical aspect ratios of ~1000 to 1. The planar geometry is also well suited to high-power diode-array pumping, either by in-plane pumping with diode bars [2], [3] or by face pumping with diode stacks [4]. In bulk materials, high-power diode pumping has been achieved via reflective pumping chambers [5], fiber coupling [6], lens ducts [7], and beam-shaping systems [8]. For fiber lasers, double-clad geometries [9] and novel v-groove designs [10] have also been employed. However, the basic geometrical compatibility between planar waveguides and high-power diode arrays can lead to significant simplification of the diode coupling scheme and, hence, to very compact laser systems. The ease of access to the guided wave in planar thin films also allows the possibility of integrating various functions, such as switching, grating reflectors and filters, polarization control, etc., in a monolithic device.

For planar waveguides, face pumping has the advantage of scalability through the area of the pumped face but suffers due to the very low single-pass pump absorption through the thin doped core layer, requiring relatively thick, and, hence, multiguided-mode, waveguides and the use of a reflective pumping chamber [4]. In-plane coupling is certainly more restricted in power, as pumping is limited to a small number of diode bars, but it still has the potential for allowing pumping levels of >100 W. The advantages of the in-plane pumping scheme include a much stronger single-pass pump absorption and compatibility with small waveguide dimensions (<10 μm) leading to high optical gains per unit pump power.

It has recently been shown that directly-bonded rare-earth-doped YAG on sapphire waveguides are well-suited to in-plane pumping by diode bars [11]. Their high numerical aperture (0.46) allows efficient coupling via fiber/rod lenses for guides with cores as small as 4 μm, despite the non-diffraction-limited nature of the fiber-lens-collimated diode pump beam. This leads to a compact overall device and output powers approaching 4 W have been obtained from a Nd:YAG/sapphire waveguide when pumped with a 20-W diode bar. However, the output of these devices is non-diffraction-limited due both to the multimode nature of the structure in the guided plane, which is necessary to efficiently capture the non-diffraction-limited diode output, and to the high Fresnel number of the monolithic cavity in the nonguided plane. Here we demonstrate diode-bar-pumped waveguide lasers that are diffraction-limited in the guided plane by the use of a double-clad, multilayer, planar waveguide structure. Such structures have previously been employed in high-power fiber lasers [12] and consist of a single-mode, rare-earth-doped lasing core surrounded by a much larger inner cladding that captures the diode pump beam. The pump light is gradually absorbed each time it passes through the doped region, and single-spatial-mode laser output is obtained. For planar guides, the size of the core, relative to the inner cladding, is much larger in order to avoid increasing the effective absorption length for the pump light beyond the practical limitations of planar fabrication. We describe how this can lead to a new regime of operation for double-clad structures where the selection of the output spatial mode is controlled by the confinement of the doping rather than the optical confinement of the core. Hence, the device works by gain mode selection rather than by cladding pumping of a single-mode core. We also show that such structures can readily be pumped by simply proximity coupling the diode bar, leading to even more compact devices (a <1 cm^2 footprint if we ignore the accompanying heatsinks and positioners) with no need for coupling optics.

This paper is organized as follows. Section II discusses the design and fabrication of the five-layer planar double-clad structures, the advantages and limitations of the high core-to-cladding size ratio regime, and how related designs are also being pursued in fiber and bulk lasers. In Section III, a double-clad Yb:YAG waveguide is characterized by Ti:sapphire end pumping, demonstrating the low propagation

Manuscript received August 23, 1999; revised October 15, 1999.

The authors are with the Optoelectronics Research Centre, University of Southampton, Highfield, Southampton SO17 1BJ, U.K.

Publisher Item Identifier S 0018-9197(00)00951-9.

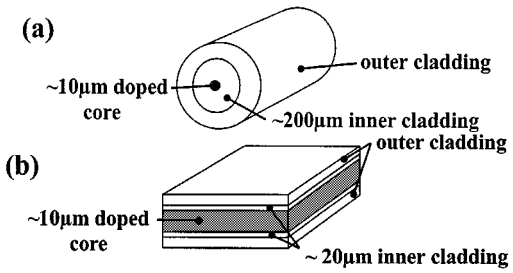

Fig. 1. Typical double-clad waveguide designs for high-power diode-pumped lasers and amplifiers in (a) fiber and (b) planar geometries.

loss, high gain, and linearly polarized diffraction-limited output mode quality of this structure. In Section IV, we describe the experimental setup for proximity coupling of diode bars to planar guides and discuss the results obtained for coupling into an 8 μm core-thickness Nd:YAG on sapphire waveguide. In Section V, we discuss the results obtained for proximity-coupled, side-pumped Nd^{3+}- and Yb^{3+}-doped YAG, double-clad waveguide structures, demonstrating multiwatt single-guided mode outputs in both cases. Finally, in Section VI, we give our concluding remarks and discuss the possibilities for also controlling the mode in the nonguided plane in order to obtain fully diffraction-limited devices.

II. Design and Fabrication of Double-Clad Planar Waveguides

Fig. 1(a) shows a typical double-clad guiding structure for high-power fiber lasers and amplifiers. The single-mode core is surrounded by a considerably larger multimode inner cladding. This, in turn, is surrounded by an outer cladding which has a much lower refractive index. In this way, the non-diffraction-limited diode pump beam can be contained in the high-numerical aperture (NA) waveguide made by the two claddings. The doped core gradually absorbs the pump radiation each time it bounces through it, leading to a much longer effective absorption length compared to bulk glass of the same doping level. Indeed, various design tricks, such as an off-center core or a noncircular inner cladding, are often used to help absorb helical pump modes which otherwise could avoid passing through the doped region at all. For a fiber, the increased length required, often to lengths of several tens of meters, is not a significant problem in terms of fabrication or increased loss. However, most planar fabrication techniques are rather limited in the length of device that can be produced and the associated propagation losses are more severe. This leads to the typical design shown in Fig. 1(b), where the low-NA single-mode doped core is a significant fraction of the overall pumped region. This, in turn, leads to an increased absorption efficiency, in both a bouncing ray model and in terms of overlap of the doped region with the guided pump modes. The rather small pumping dimension is not a problem for the planar geometry because we have no requirement to circularize the diode beam and we can take advantage of its near-diffraction-limited nature in the fast axis. The drawback to this design is the possibility of a significant overlap of the higher order modes of the inner-cladding waveguide with the gain region, increasing the possibility of a non-diffraction-limited output.

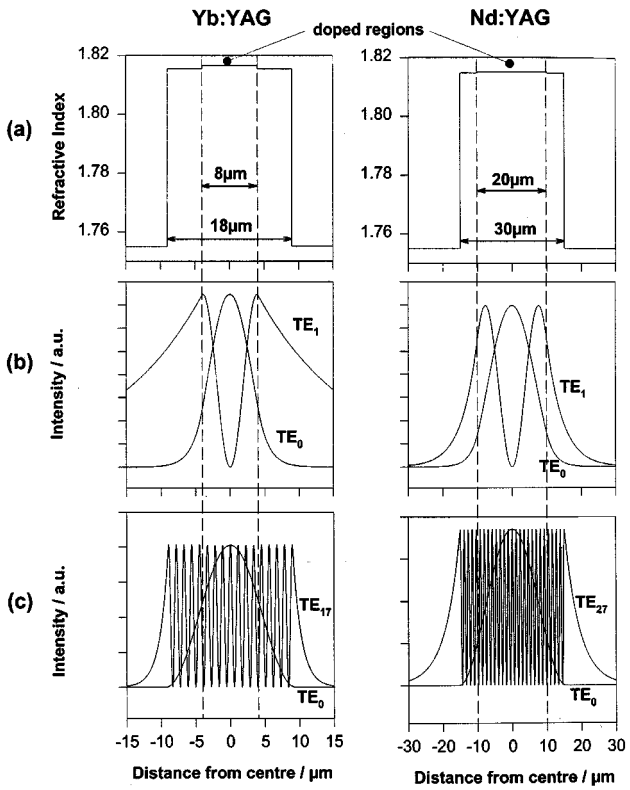

Fig. 2. The five-layer refractive index profiles for (a) the double-clad Yb^{3+}- and Nd^{3+}-doped waveguides and theoretical mode profiles for (b) the three-layer core and (c) cladding waveguides.

The waveguides used in our experiments were fabricated by Onyx Optics, Inc., by the direct-bonding method [11], [13]. This technique allows precision-polished materials to be joined together by van der Waals intermolecular forces, with bond strengths sufficient to withstand further polishing down to layer thicknesses of a few micrometers. This allows the production of multilayer waveguides with bulk optical properties and low propagation losses. Fig. 2(a) shows the dimensions and refractive index profiles for the double-clad waveguides used in the following laser experiments. The outer cladding is made of sapphire oriented to the (001) direction parallel to the plane of the waveguide core and in the direction of propagation for the laser output. This material is very durable, polishes well, and has a high thermal conductivity. The inner cladding is made of undoped YAG, which again has good mechanical and thermal properties and is known to bond well to sapphire [11]. This outer guidance structure has an NA of ~0.46 which is sufficient to optically confine the highly divergent output from a typical diode bar, when proximity coupled to the waveguide. The core consists of rare-earth-doped YAG, which is the standard high-power solid-state laser material. Guidance in the core region can arise from the increase in refractive index associated with the rare-earth doping. Table I gives the relevant index values used for our design which were taken from [14]–[17]. The values used for the increase in index due to the doping are based on measurements taken at 633 nm, but it is has been observed that this index difference does not change dramatically with wavelength [16], and so should still be valid out to 1.1 μm.

TABLE I
REFRACTIVE INDICES OF THE WAVEGUIDE STRUCTURE AT VARIOUS WAVELENGTHS OF INTEREST.

Refractive Indices at Pumping and Lasing Wavelengths				
	808nm	941nm	1029nm	1064nm
Sapphire (n_o) [13]	1.760	1.757	1.755	1.755
YAG [14]	1.8212	1.8175	1.8154	1.8147
10at.% Yb:YAG [15]	-	1.8187	1.8166	-
1at.% Nd:YAG [16]	1.8216	-	-	1.8151

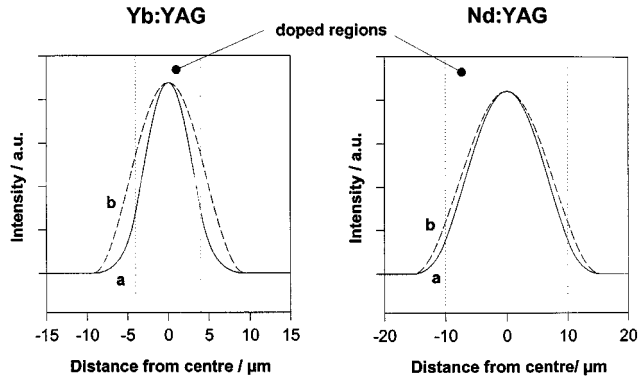

(a) (b)

Fig. 3. The theoretical fundamental mode profiles for the five-layer structures (a) with and (b) without allowing for the index increase due to the rare-earth doping.

Fig. 2(b) shows the predicted propagation modes (in this case, TE modes) at the laser wavelength for the core waveguide, assuming an infinite inner cladding layer thickness. It can be seen that both waveguides allow two propagation modes and, in both cases, the fundamental mode has nearly, but not fully, decayed by the time it reaches the outer cladding layer. Fig. 2(c) shows predicted TE modes at the laser wavelengths for the inner cladding guide assuming an infinite outer cladding layer and that there is no index change in the core due to the rare-earth doping. In both cases, the fundamental mode and the highest- order mode are shown (the Nd^{3+}-doped structures support 28 modes and the Yb^{3+}-doped structure supports 18). It can clearly be seen that the higher order modes of the cladding guide have a substantial overlap with the gain region and, if the guide was doped throughout the cladding guide, we would expect a multimode laser output. However, the fundamental mode has the best overlap with the confined doped region, and the smallest mode size, and so should reach laser threshold first. Due to the confinement of the doped region, the fundamental mode can saturate all the available gain, stopping the higher order modes from reaching threshold, and, hence, a single-mode output is obtained. The fundamental mode in question should be that of the overall five-layer structure, rather than those shown in Fig. 2, because the core modes still have a noticeable mode intensity at the boundary with the outer cladding layer. A question then arises as to whether the index change associated with the doping is of any importance at all. Fig. 3 shows a comparison of the fundamental modes of the five-layer structures (a) with and (b) without this small index rise. It can clearly be seen that the index rise leads to a stronger confinement of the mode to the doped region. This will lower its threshold but could make it harder for it to saturate the gain fully. A brief summary of the theory used to calculate the mode profiles described in this section is given in the Appendix.

Thus, we can see that this is a new operating regime for double-clad lasers that is not strictly the same as that described as cladding pumping where the core size is much smaller than the inner cladding and the lasing mode is truly associated with the core guiding structure. This new regime could perhaps be more accurately described as gain mode selection, and it begins when the mode of the core starts to have appreciable intensity at the boundary with the outer cladding region. Clearly, if the core-to-cladding-size ratio is pushed near to 1, the higher order modes will start to see unsaturated gain and could start to lase, but we will experimentally demonstrate in Section V that ratios of 0.67 for Nd:YAG and 0.44 for Yb:YAG give single-mode laser outputs. The advantage of such high ratios is the increased absorption efficiency. As we have already stated, this is of particular relevance to planar devices, but large mode areas can also be of interest in high-power pulsed fiber lasers in order to increase energy storage capabilities. This has already inspired work on large-mode-area fibers [18] where the fundamental mode of a multimode core is selected by only doping the central region. A cladding-pumped version of this fiber design has also recently been reported [19], but in this case the mode selection is still strictly from amongst those associated with the core rather than the overall structure. However, it is possible that the desire for further increases in power could push double-clad fiber lasers into the high core-to-cladding ratio regime. It is also interesting to note that a core-doped bulk laser, also made by direct bonding, has recently been demonstrated which shows enhanced beam quality over a uniformly doped rod [20]. In this case, mode selection occurs between those allowed by the optical resonator rather than those allowed by a multimode waveguide.

III. Ti-SAPPHIRE PUMPED DOUBLE-CLAD Yb:YAG WAVEGUIDE LASER

In order to characterize the novel double-clad structures in terms of propagation loss, gain, polarization behavior, and mode quality, the end-pumped laser performance of the Yb^{3+}-doped guide described in Section II was assessed using a Ti:sapphire pump laser. The 5 mm $\times$ 10 mm guide had its end-faces polished plane and parallel. An estimate of the absorption length for 10 at.% Yb^{3+}-doped YAG was made from the results of Lacovara *et al.* [21], giving values of ~1.1 mm at 941 nm and 968 nm, and ~1.9 mm at 915 nm. For Ti:sapphire pumping, we chose to use the weaker absorption at 915 nm due to the pump laser having a greater output power at this wavelength. A rough estimate of the absorption length for the double-clad guide was made by increasing this figure according to the ratio of the undoped to doped areas of the pumped region. Thus, we expected an absorption length of 4.3 mm, which allowed us to choose to pump the waveguide along the 5-mm-long direction. This simple estimation of absorption length is expected to be a good approximation for our structures because, in contrast to the case of some fiber double-clad geometries, it is hard to envisage pump modes

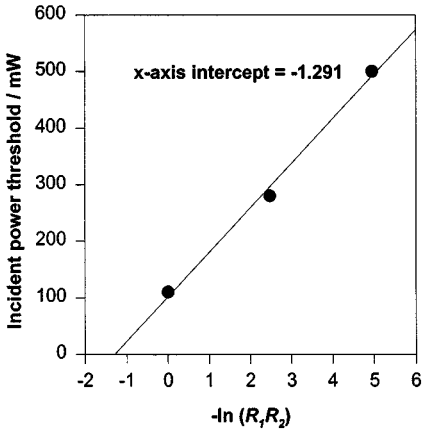

Fig. 4. Incident power threshold against $-\ln(R_1R_2)$. The intercept on the x axis is related to the round-trip loss.

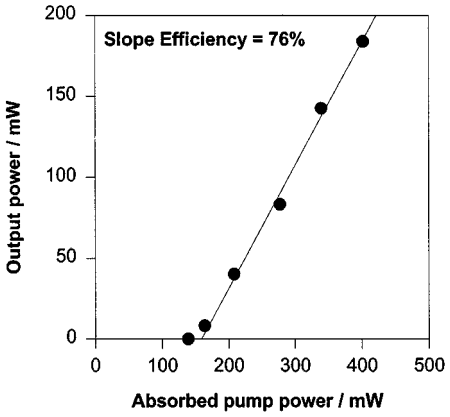

Fig. 5. Output power against absorbed pump power for the Ti:sapphire pumped Yb:YAG double-clad waveguide laser.

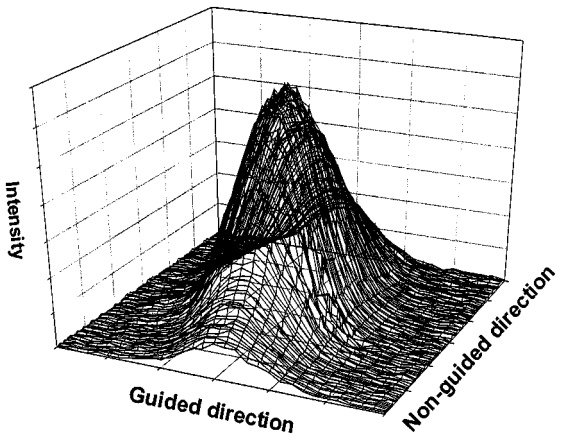

Fig. 6. Imaged single-mode diffraction-limited output of the Yb:YAG double-clad waveguide laser.

which could propagate without a substantial overlap with the doped region.

The laser resonator was formed by the end-faces of the waveguide with the addition of butted plane mirrors as required. Initially, using a X6 microscope objective, we took care to couple the pump light into the waveguide such that propagation of a fundamental pump mode was observed by imaging the output onto a CCD camera. The 1.029-μm lasing threshold was then determined as a function of the output coupling. The use of only Fresnel reflections (8.4%) or highly reflective (HR) mirrors helps to avoid possible etalon effects between the end-faces and the butted mirror, causing an effective output coupling different to the normal transmission of the mirror. The fact that lasing occurred off the bare end-faces of the waveguide at a threshold of just 500-mW incident power demonstrates the high gain available from the waveguide configuration (in this case, a round-trip gain of 21.5 dB). Assuming that the laser has the same mode size in each case, and that there is no change in losses with changing pump intensity, the threshold $P_{\rm th}$ should obey the following equation:

$$P_{\rm th} = k(2\sigma_a N_1 l - \ln(R_1R_2) + 2\alpha l)$$

where k is a constant dependent upon the material parameters, the pump launch efficiency, and the pump and signal spatial properties, σ_a is the absorption cross section at the laser wavelength, N_1 is the lower laser level population density, l is the length of the cavity, R_1 and R_2 are the mirror reflectivities, and α is the propagation loss coefficient. Therefore, a plot of the threshold versus $-\ln(R_1R_2)$ should have an intercept on the $-\ln(R_1R_2)$ axis of $-(2\sigma_a N_1 l + 2\alpha l)$. Such a plot is shown in Fig. 4. Using $\sigma_a = 1.8\times10^{-24}$ m^2, $N_1 = 6.9\times10^{25}$ m^{-3} (5% of the total population) and $l = 5\times10^{-3}$ m, we find a value for α of 5 m^{-1} or equivalently 0.2 dB/cm. Thus, this five-layer waveguide has losses equivalent to those found for previously fabricated two-layer direct-bonded waveguides [11], [13].

The focusing of the Ti:sapphire pump laser was then changed by using a 5-cm focal-length lens instead of the X6 objective. When viewed on the CCD camera, it was clear that we were now coupling to the higher order modes of the five-layer structure, as we would with a high-power diode laser. Under these conditions, the combined launch and absorption efficiency was calculated to be 0.77 by comparing the measured pump power before and after the guide. Taking into account the rough estimate of the absorption length made above, we can estimate that this corresponds to a near 100% launch efficiency, which is not surprising for such a large and high NA waveguide pumped by a Ti:sapphire laser. The output efficiency and mode quality was tested using a cavity formed by one HR mirror and one bare end-face of the waveguide. The results are shown in Fig. 5. The high slope efficiency of 76% (59%) with respect to absorbed (incident) power is in-line with what may be expected for Yb (the quantum limit for 915-nm pumping is 89%), but it is another indication of the high quality of the double-clad waveguide. The mode profile of the lasing output was investigated using both a CCD camera and a Coherent M^2 meter. No matter how badly we attempted to launch the pump light in order to propagate high-order pumping modes, we were only able to see a single-mode waveguide laser output. The output intensity profile imaged onto the CCD camera is shown in Fig. 6. The clean single-lobed output is not, in itself, proof of a single-mode diffraction-limited behavior, but, when M^2 measurements were taken, a value of 1.2 was found in the guided direction. In fact, in this case, the M^2 value in the nonguided direction was also near 1.0, and so we have a truly diffraction-limited output. However, as will be shown in the later sections, diode-array pumping

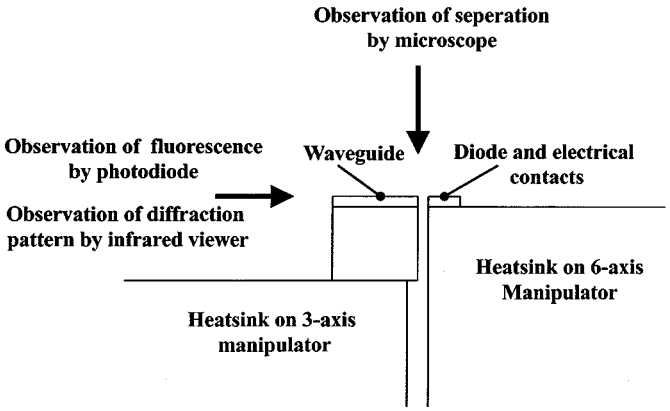

Fig. 7. Experimental arrangment for proximity coupling.

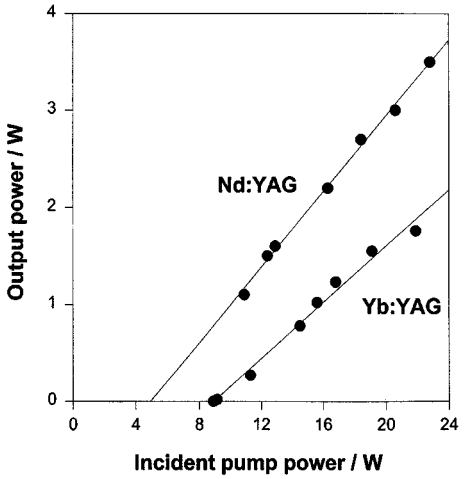

Fig. 8. Output power versus incident pump power for the double-clad proximity-side-pumped Yb:YAG and Nd:YAG waveguides.

would lead to a much larger gain region in this nonguided plane and hence to a multimode output. The output was at 1.029 μm, which is at the peak of the Yb emission spectrum, and was found to be TE polarized. The linearly polarized output is in contrast to the randomly polarized output previously observed with two-layer YAG on sapphire guides and is perhaps an indication of increased stress in the five-layer structures, leading to a difference in TM and TE propagation losses and/or mode sizes that is sufficient to give a polarized laser emission. At present, it is not known if such effects are responsible for this behavior, but in practice this is a very convenient way of obtaining a polarized output which may be useful for future application to nonlinear frequency conversion.

IV. Proximity Coupling

For our first demonstration of proximity coupling, we used a waveguide consisting of an 8-μm-thick Nd:YAG core contact-bonded to a sapphire substrate. The guide was 18 mm long by 2 mm wide and was end-polished on all four faces to allow lasing along the long axis and pumping along the short axis. This pumping region is much thinner than would be the case for a double-clad structure and so represents a strong test of the capabilities of the proximity coupling technique. The 807-nm Jenoptik diode bar had an output power of 10 W and a 1 cm by 1 μm emission aperture. Fig. 7 shows the experimental apparatus used to achieve proximity coupling. The diode and waveguide are mounted on separate water-cooled heatsinks and these are held on their own manipulators. The diode can easily be brought to within a few tens of micrometers of the waveguide by observation of their separation with a microscope. They can then be aligned to have the same separation across the length of the diode and, by observing the diffraction pattern, their relative orientations can be corrected such that they are parallel to each other. Observation of the fluorescence intensity allows the relative heights to be adjusted. The diode and waveguide are then moved closer, taking care to make any further small corrections in their orientations, until optimum laser output is achieved. By measuring the pump power before and after the waveguide and accounting for Fresnel reflections, a combined launch and absorption efficiency factor of 0.45 was deduced. Using a bulk piece of Nd:YAG with the same doping level, an absorption length of 3 mm was measured for a similar diode. Thus, we arrive at a proximity-coupling launch efficiency of nearly 90%. It is clear that this is not only a simple and compact coupling scheme but it is also very efficient when used for high-NA (0.46) guides, even for sub-10-μm core widths. Observation of the fluorescence intensity showed that it gradually increased, with interferometric-like fluctuations, as the diode approached the waveguide and that it became steady when contact was made. However, it was not clear whether this contact was between the waveguide and the diode facet or another part of the surrounding contacts as it was difficult to tell if the facet was slightly recessed or not. Optimum laser performance did not necessarily occur at this contacted point.

The side-pumped laser performance of the guide was quickly tested by butt-coupling an HR and a 77% R mirror to the end-faces of the waveguide. Over 0.5 W of laser output was obtained for 6 W of incident power but, as would be expected, it was highly multimode. Indeed, in the nonguided direction, it was observed that lasing paths involving reflections off the polished side faces of this long thin guide were occurring. Nevertheless, our primary aim of demonstrating the feasibility of proximity coupling had been achieved.

V. Proximity-Coupled, Diode Bar Side-Pumped, Nd^{3+}- and Yb^{3+}-Doped YAG, Double-Clad Waveguide Lasers

The 1 cm long by 5 mm wide, double-clad, Nd^{3+}- and Yb^{3+}-doped guides described in Section II were side-pumped by 20-W diode bars, at 807 nm and 941 nm, respectively, using the same proximity coupling setup as described in Section V. Due to the larger overall pumping areas, the alignment was found to be easier than for the 8-μm core-pumped waveguide described earlier. Fig. 8 shows the laser output power versus incident pump power for both lasers. For the Yb-doped sample, an upper limit to the combined launch and absorption efficiency factor was measured to be 63% by measuring the pump power before and after the waveguide. This was an upper limit as we were not able to catch all the pump light after the waveguide. We would expect the launch efficiency to be near 100% and so the 5-mm width of the double-clad waveguide appears to be approximately one absorption length for the diode pump.

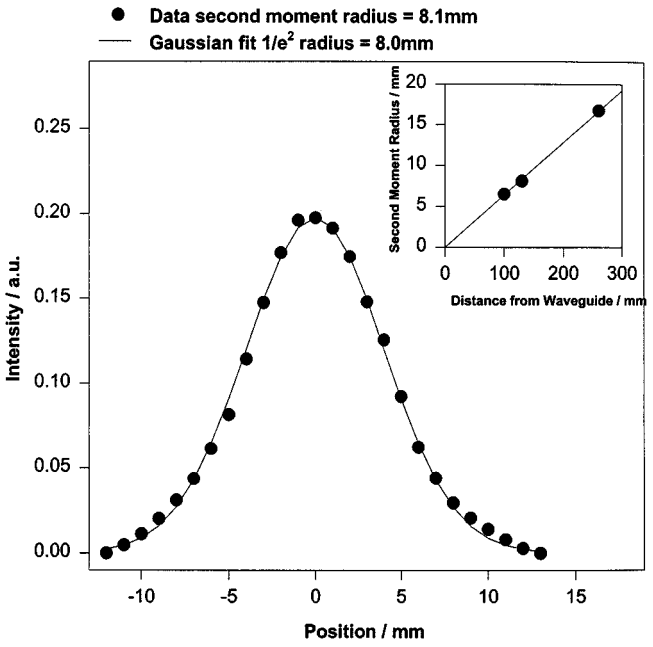

Fig. 9. Measured far-field intensity profile for the Yb:YAG waveguide laser in the guided direction with a Gaussian fit. Inset is the measured second moment radius at various distances form the waveguide output.

The Yb laser results were taken using a 7% output coupler and show a 14.5% slope efficiency with respect to incident power, and hence (also accounting for one Fresnel reflection) a slope efficiency of $\geq$23% with respect to absorbed power. With optimization at the high pump level, a maximum output power of 2.2 W was obtained, but attempts to increase the output power by using a mirror to reflect any left over pump light back into the waveguide were unsuccessful. The output wavelength in this case was found to be around 1048 nm, corresponding to the transition to the highest Stark level of the $^4F_{7/2}$ ground level. While this transition has a much lower emission cross section than the 1029-nm line, it also suffers less from ground state absorption and so can quite easily be made to lase [22]. The output was found to be TE polarized as had previously been observed with Ti:sapphire pumping. The far-field output profile of the beam in the guided direction was measured by scanning the vertical intensity profile of one section of the output. Fig. 9 shows that the results fit well to a Gaussian profile and that measuring the second moment radius at various distances from the guide gives a divergence of 64.1 mrad. The calculated radius of the fundamental mode of the Yb:YAG double-clad guide is 5.26 μm which would lead to an output divergence of 63.4 mrad, suggesting that the output is indeed in the fundamental mode and has an M^2 value very close to 1. The output mode is still highly multimode, although single-lobed, in the nonguided plane. This is as we expect due to the large gain area and, as yet, no attempt has been made to control the mode in this direction.

Fig. 8 also shows the output performance of the Nd:YAG double-clad structure using a 60% reflectivity output coupler. It can be seen that this laser has a lower threshold (~5 W) and a higher slope efficiency with respect to incident power (~20%) than the Yb:YAG laser. With optimization at the maximum pump power, an output power of ~4 W was obtained. Once again, the output divergence is consistent with a fundamental guided-mode output. In this case, the output is at 1.064 μm and was found to be TE polarized. The reduced efficiency compared to the Ti:sapphire end-pumped results is to be expected due to the worse spatial overlap of a side-pumped configuration [23]. The use of coated end-faces, instead of mirrors butt-coupled to the waveguide with fluorinated liquid, may also help to improve output powers.

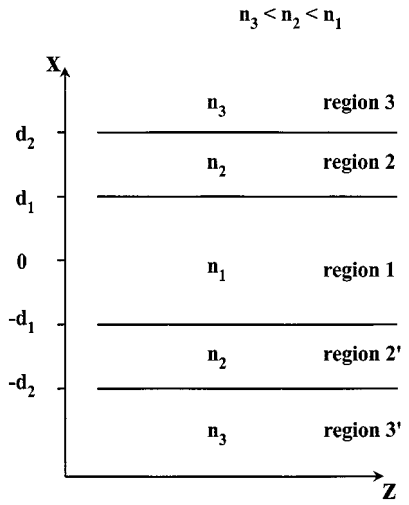

Fig. 10. Symmetric five-layer waveguide model.

VI. Conclusion

We have demonstrated the first double-clad planar waveguide lasers based on Nd^{3+}- and Yb^{3+}-doped YAG. These structures give a single guided-mode multiwatt output when pumped by high-power diode bars. The desire to keep the device to maximum dimensions of ~1 cm has led to a high core-to-cladding size ratio and mode selection occuring due to the confinement of the gain rather than the cladding pumping of a single-mode core, as is normally the case in fiber lasers. We have also shown that such structures are well-suited to proximity-coupled diode pumping, which leads to very compact devices where the diode and waveguide footprint is $<$1 cm^2. Work in the immediate future will concentrate on obtaining outputs that are also diffraction-limited in the nonguided plane. Here the problem is to couple the broad gain area to a single spatial mode without compromising the simple monolithic nature of our current devices. Routes to this end could include two-dimensional double-clad structures, unstable resonators, and adiabatic tapers. The introduction of passive Q-switching sections is also of great interest for the near future. It is our aim to develop such technologies and combine them with the highly compact and simple devices produced to date.

Appendix I

This section describes the modeling of the propagation modes of a five-layer symmetric waveguide. Fig. 10 shows the modeled structure. It is to be expected that symmetric (even) and asymmetric (odd) field solutions will exist due to the symmetry of the structure. The mode effective indices will lie between n_1 and n_3 and so we would expect exponential decay in region 3, oscillatory behavior in region 1, and both in region 2 (as the effective

$$E_y = \begin{pmatrix} \left(\frac{2\alpha_2}{\alpha_2+\alpha_3}\right)e^{-d_2(\alpha_2-\alpha_3)}e^{-\alpha_3 x} & \text{region } 3 \\ e^{-\alpha_2 x} + \left(\frac{\alpha_2-\alpha_3}{\alpha_2+\alpha_3}\right)e^{-2d_2\alpha_2}e^{\alpha_2 x} & \text{region } 2 \\ \left[e^{-\alpha_2 d_1} + \left(\frac{\alpha_2-\alpha_3}{\alpha_2+\alpha_3}\right)e^{-\alpha_2(2d_2-d_1)}\right]\begin{bmatrix}\cos(k_1x)/\cos(k_1d_1)\\ \sin(k_1x)/\sin(k_1d_1)\end{bmatrix} & \text{region } 1 \\ \pm\left(e^{\alpha_2 x} + \left(\frac{\alpha_2-\alpha_3}{\alpha_2+\alpha_3}\right)e^{-2d_2\alpha_2}e^{-\alpha_2 x}\right) & \text{region } 2' \\ \pm\frac{2\alpha_2}{\alpha_2+\alpha_3}e^{-d_2(\alpha_2-\alpha_3)}e^{\alpha_3 x} & \text{region } 3' \end{pmatrix} e^{-ik_z z}$$

index can be greater or smaller than n_2). With this in mind, we choose the TE field solutions below:

$$E_y = \begin{pmatrix} A_3 e^{-\alpha_3 x} & \text{region } 3 \\ A_2 e^{-\alpha_2 x} + A_2' e^{\alpha_2 x} & \text{region } 2 \\ A_1\begin{bmatrix}\cos(k_1x)\\ \sin(k_1x)\end{bmatrix} & \text{region } 1 \\ \pm(A_2 e^{\alpha_2 x} + A_2' e^{-\alpha_2 x}) & \text{region } 2' \\ \pm A_3 e^{\alpha_3 x} & \text{region } 3' \end{pmatrix} e^{-ik_z z}$$

where the upper and lower solutions correspond to the even and odd modes. Dispersion relations for the mode constants k_z, k_1, α_2, and α_3 can be obtained by applying the wave equation in the five regions, and the relative field amplitudes A_n can be found by applying the boundary conditions of continuity to the electric and magnetic fields [24]. In this way, we arrive at the field expressions shown at the top of the page and the guidance conditions

$$\begin{bmatrix}\tan\\ \cot\end{bmatrix}(k_1 d_1) = \pm\frac{\alpha_2}{k_1}\left(\frac{\alpha_3 + \alpha_2\tanh[\alpha_2(d_2-d_1)]}{\alpha_2 + \alpha_3\tanh[\alpha_2(d_2-d_1)]}\right).$$

It can be seen that the guidance condition reduces to the normal three-layer expression [23] by setting $d_1 = d_2$.

ACKNOWLEDGMENT

The authors would like to acknowledge R. J. Beach and H. E. Meissner for useful discussions. The Optoelectronics Research Centre is an EPSRC (U.K.) interdisciplinary research centre.

REFERENCES

[1] W. Koechner, *Solid-State Laser Engineering*, 4th ed. Berlin, Germany: Springer-Verlag, 1996, ch. 7.
[2] U. Griebner, H. Schönnagel, R. Grunwald, and S. Woggon, "Transversely guided pumped Yb:YAG laser," in *Tech. Dig. Conf. Lasers and Electro-Optics*, 1997, pp. 307–308.
[3] C. L. Bonner, C. T. A. Brown, D. P. Shepherd, W. A. Clarkson, A. C. Tropper, and D. C. Hanna, "Diode-bar end-pumped high-power Nd:$Y_3Al_5O_{12}$ planar waveguide laser," *Opt. Lett.*, vol. 23, pp. 942–944, 1998.
[4] A. Faulstich, H. J. Baker, and D. R. Hall, "Face pumping of thin, solid-state slab lasers with laser diodes," *Opt. Lett.*, vol. 21, pp. 594–596, 1996.
[5] J. J. Chang, E. P. Dragon, C. A. Ebbers, I. L. Bass, and C. W. Cochran, "An efficient diode-pumped Nd:YAG laser with 451 W of CW IR and 182 W of pulsed green output," in *OSA TOPS on Advanced Solid-State Lasers*, 1998, pp. 300–304.
[6] M. Karszewski, U. Brauch, K. Contag, S. Ergard, A. Giesen, I. Johannsen, C. Stewart, and A. Voss, "100 W TEM_{00} operation of Yb:YAG thin disc laser with high efficiency," in *OSA TOPS on Advanced Solid-State Lasers*, 1998, pp. 296–299.
[7] R. J. Beach, "Theory and optimization of lens ducts," *Appl. Opt.*, vol. 35, pp. 2005–2015, 1996.
[8] W. A. Clarkson and D. C. Hanna, "Two-mirror beam-shaping technique for high-power diode bars," *Opt. Lett.*, vol. 21, pp. 375–377, 1996.
[9] E. Snitzer, H. Po, F. Hakimi, R. Tumminelli, and B. C. McCollum, "Double-clad, offset core Nd fiber laser," presented at the Conference on Optical Fiber Communication, paper PD5, 1988.
[10] M. Hofer, M. E. Fermann, and L. Goldberg, "High-power side-pumped passively mode-locked Er-Yb fiber laser," *IEEE Photon. Technol. Lett.*, vol. 10, pp. 1247–1249, 1998.
[11] D. P. Shepherd, C. L. Bonner, C. T. A. Brown, W. A. Clarkson, A. C. Tropper, D. C. Hanna, and H. E. Meissner, "High-numerical-aperture, contact-bonded, planar waveguides for diode-bar-pumped lasers," *Opt. Commun.*, vol. 160, pp. 47–50, 1998.
[12] V. Dominic, S. MacCormack, R. Waarts, S. Sanders, S. Bicknese, R. Dohle, E. Wolak, P. S. Yeh, and E. Zucker, "110 W fiber laser," presented at the Conf. on Lasers and Electro-Optics/Europe, post-deadline paper CPD11, 1999.
[13] C. T. A. Brown, C. L. Bonner, T. J. Warburton, D. P. Shepherd, A. C. Tropper, D. C. Hanna, and H. E. Meissner, "Thermally bonded waveguide lasers," *Appl. Phys. Lett.*, vol. 71, pp. 1139–1141, 1997.
[14] D. N. Nikogosyan, *Properties of Optical and Laser-Related Materials*. Chichester, U.K.: Wiley, 1997, p. 5.
[15] D. E. Zelmon, D. L. Small, and R. Page, "Refractive-index measurements of undoped yttrium aluminum garnet from 0.4 to 5.0 μm," *Appl. Opt.*, vol. 37, pp. 4933–4935, 1998.
[16] F. Patel, "Refractive index measurements of Yb:YAG," Univ. California, private communication.
[17] D. Pelenc, "Guide d'onde laser en Nd:YAG et Yb:YAG per E.P.L.," Ph. D. dissertation, Département Optronique du LETI, Grenoble, France, 1992.
[18] H. L. Offerhaus, N. G. Broderick, D. J. Richardson, R. Sammut, J. Caplen, and L. Dong, "High-energy single-transverse-mode Q-switched fiber laser based on a multimode large-mode-area erbium-doped fiber," *Opt. Lett.*, vol. 23, pp. 1683–1685, 1998.
[19] H. L. Offerhaus, J. A. Alvarez-Chavez, J. Nilsson, P. W. Turner, W. A. Clarkson, and D. J. Richardson, "Multi-mJ, multi-Watt Q-switched fiber laser," presented at the Conf. on Lasers and Electro-Optics, post-deadline paper CPD10, 1999.
[20] A. Lucianetti, R. Weber, W. Hodel, H. P. Weber, A. Papashvili, V. A. Konyushkin, and T. T. Basiev, "Beam-quality improvement of a passively Q-switched Nd:YAG laser with a core-doped rod," *Appl. Opt.*, vol. 38, pp. 1777–1783, 1999.
[21] P. Lacovara, H. K. Choi, C. A. Wang, R. L. Aggarwal, and T. Y. Fan, "Room-temperature diode-pumped Yb:YAG laser," *Opt. Lett.*, vol. 16, pp. 1089–1091, 1991.
[22] D. Pelenc, B. Chambaz, I. Chartier, B. Ferrand, C. Wyon, D. P. Shepherd, D. C. Hanna, A. C. Large, and A. C. Tropper, "High slope efficiency and low threshold in a diode-pumped epitaxially-grown Yb:YAG waveguide laser," *Opt. Commun.*, vol. 115, pp. 491–497, 1995.
[23] D. C. Hanna, A. C. Large, D. P. Shepherd, A. C. Tropper, I. Chartier, B. Ferrand, and D. Pelenc, "A side-pumped Nd:YAG epitaxial waveguide laser," *Opt. Commun.*, vol. 91, pp. 229–235, 1992.
[24] D. L. Lee, *Electromagnetic Principles of Integrated Optics*, New York: Wiley, 1986, ch. 4.

C. L. Bonner, photograph and biography not available at the time of publication.

T. Bhutta, photograph and biography not available at the time of publication.

D. P. Shepherd, photograph and biography not available at the time of publication.

A. C. Tropper (M'98), photograph and biography not available at the time of publication.